Enhancement of Classification Accuracy Using Conflation Procedures

Howard Veregin
Department of Geography, University of Minnesota
267-19th Ave. S.
Minneapolis, Minnesota, USA 55455

Peter Sincák
Computational Intelligence Group, Laboratory of AI
Department of Cybernetics and Artificial Intelligence
Technical University of Kosice
Letna, 9, 04200 Kosice, Slovak Republic

Norbert Kopco
Computational Intelligence Group, Laboratory of AI
Department of Cybernetics and Artificial Intelligence
Technical University of Kosice
Letna, 9, 04200 Kosice, Slovak Republic

Abstract

This study focuses on conflation procedures to enhance classification accuracy for remote sensing imagery. In this context, conflation refers to the merging of the most accurate portions of a set of classified images to yield a result that is more accurate than any individual image. Two main types of conflation procedures are discussed. The first is a heuristic approach based on if-then rules and the second is based on statistical manipulation of misclassification probabilities. The conflation procedures are tested on three classified images derived from a high-resolution multispectral video mosaic using non-traditional classification methods. For these test data, conflation yields improvements in classification accuracy of up to 15 percent.

Introduction

Classification is one of the most basic image processing operations. It involves a transformation of pixel spectral response values to extract various cover classes. An enormous volume of literature exists on this topic and numerous classifiers have been developed and applied to remote sensing imagery (Swain and Davis, 1978). For supervised classification the best-known technique is Bayesian classification based on the a priori assumption of a Gaussian distribution of training data (Tou and Gonzales, 1974). For unsupervised classification the main methods include ISODATA and other types of clustering (Ocelikova, 1993, 1994). Significant progress in classification has also been made using fuzzy logic and neural networks (Benediktsson *et al.*, 1990; Hepner *et al.*, 1990). Neural-based classification of remote sensing images has been reported in Heerman and Khazenie (1992), Kulkarni (1994), Civco and Wang (1994), Foody *et al.* (1995) and Carpenter *et al.* (1997). Applications of fuzzy systems in pattern recognition can be found in Wang (1990) and Pao (1989). A large number of experiments have also been done with neuro-fuzzy approaches to classification problems (Lin and Lee, 1996). Wilkinson (1995) provides a methodological discussion about the future of classification approaches in remote sensing.

In the present study, the classification problem is examined with specific reference to high-resolution video imagery of urban areas. Video is a relatively new data source for remote sensing and has promise for a wide range of applications (King, 1995). For urban applications, the main advantage of video data is that it provides sufficient resolution for detailed analysis of urban land cover. No existing commercial satellite system provides multispectral imagery with a comparable pixel size at a comparable price (although several systems are slated for deployment in the near future).

High-resolution urban imagery presents some unique challenges for the classification process. Such imagery contains high within-class variation in spectral response as a result of the small pixel size coupled with the spatial complexity of the urban scene. Previous research shows that as resolution is enhanced classification accuracy often declines for classes exhibiting a high degree of internal variability

(Markham & Townshend, 1981; Toll, 1985; Cushnie, 1987). Traditional statistical classifiers are often unsuccessful in this context due to the difficulty of discriminating among classes in feature space (Veregin *et al.*, 1995). Non-traditional classifiers based on neural nets and fuzzy sets appear to be only marginally better (Sincak *et al.*, 1998).

In the present study we develop, implement and evaluate a set of "conflation" procedures for enhancing classification accuracy. We use the term conflation to refer to a process in which alternate classifications of the same area are merged to produce a hybrid image containing the most accurate portions of the classification alternatives. This approach exploits the fact that different classifiers often exhibit significant differences in per-class accuracy statistics. Classes that are inaccurately depicted on one image are often quite accurate on another. By conflating a set of images, one extracts the most accurate parts of each rather than searching for a single optimal classifier that performs well for all classes.

The term conflation generally refers to any procedure involving data merging and integration. For example, in image processing one might integrate imagery with high spatial resolution and imagery with high spectral resolution to produce a hybrid image. In GIS (geographic information systems) competing digital representations of the same features might be evaluated with respect to their reliability in order to produce a hybrid database from the most reliable pieces (Goodchild, 1996). Our conflation approach has certain commonalities with rule-based classification, except that we use only internal evidence (i.e., misclassification patterns present in the data) and do not rely upon expert knowledge or ancillary data. There are also parallels with evidential reasoning (Baldwin *et al.*, 1995), and in particular the notion of an "evidential interval." The evidential interval describes the disparity between the degree of support for a hypothesis and the degree to which the available evidence does not refute the hypothesis. In the context of image classification, support for a given hypothesis is a measure of the probability that a pixel belongs to a particular class; the approach can therefore be used to assess support for competing hypotheses (alternate class assignments for a pixel) based on one or more data sources. Lee *et al.* (1987) provide a remote sensing application in which this approach is used to provide information about the composition of mixed classes.

In this study we apply conflation to a 1-meter multispectral urban video image classified using several non-traditional approaches — modular neural networks, fuzzy ARTMAP and supervised classification based on fuzzy sets. We first outline the results of these classifiers and then describe and evaluate the conflation procedures.

Data

Our study area is portion of the Mud Run Creek urban watershed in southwest Akron, Ohio (Figure 1). Our ultimate objective is to use remote sensing to derive permeability data for input to urban storm water runoff models (Veregin *et al.*, 1995). The first step in this process is accurate delineation of land cover types. The Mud Run Creek study area is over 1000 ha in size and is composed of multiple land uses ranging from open space to developed commercial and residential zones. Subcatchments of the Mud Run Basin were delineated on the basis of topography and linkages in the storm sewer drainage network. Several subcatchments were selected for detailed analysis and one of these, subcatchment 24, is the focus of this study. The area of this subcatchment is approximately 50 ha.

Video imagery was obtained on December 30, 1994, under cloud-free skies at near-noon local time. There was no snow cover and tree foliage was absent, giving an unrestricted view of actual ground cover. Imagery was acquired with a color video camera recording onto video tape. Altitude was approximately 1625 m AGL, giving a pixel size of approximately 1 m. Video imagery was post-processed by digitizing the red, green and blue bands from selected video frames, yielding a vector of RGB values in the range 0-255 for each pixel. Adjacent frames within subcatchment 24 were mosaiced digitally using ground control points derived from large-scale engineering maps. At this stage, the imagery was also resampled to produce exact 1-m resolution. The digital mosaic was then cropped to conform to the dimensions of subcatchment. The mosaic contains 420 rows and 1100 columns of pixels, giving 462,000 pixels in each band.

Land cover classes were identified in the field by the investigators and their students. Representative samples were marked on maps and then transferred to the video image for digital delineation. Refinement of the classes, including the addition of the class "shadow" and the merging of spectrally-similar classes, was carried out at this time.

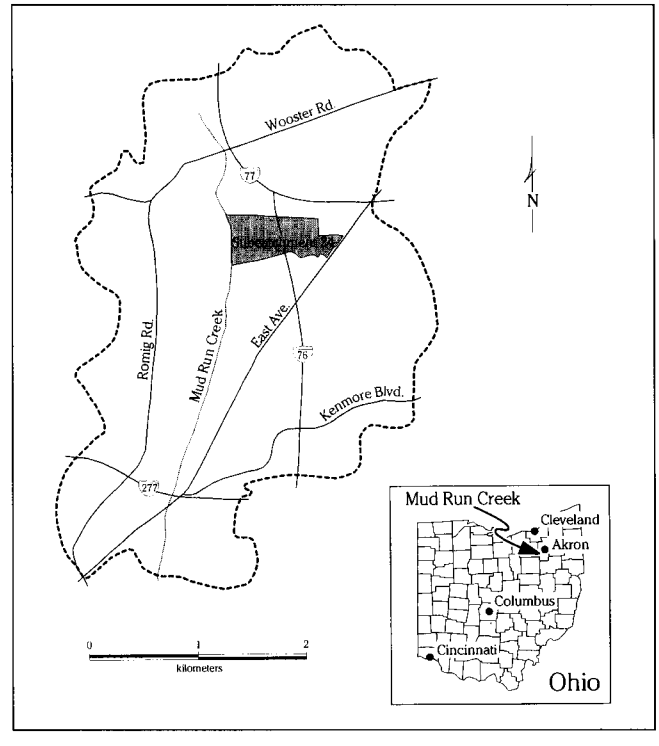

Figure 1 Study area.

The final set of eight classes are as follows:

- Deciduous trees
- Grass
- Grass-stubble
- Water
- Asphalt
- Concrete
- Shingle roofs
- Shadow

These classes are spectrally meaningful given the spatial and spectral resolution of the sensing system and the degree of spatial variability in the subcatchment. Note that these classes are "physical" rather than "interpreted." In other words, the classes represent actual physical ground cover types (such as "concrete") rather than abstract categories (such as "residential") defined by particular mixtures of physical cover types. Of course, any set of classes is meaningful within a specific range of spatial resolution levels. Our physical classes cannot be resolved with lower-resolution satellite imagery, just as the interpreted categories visible on satellite images cannot be resolved on 1-m video data. Higher resolution would have allowed us to delineate even more detailed classes but the classes we have extracted are well-suited to our purposes.

Classification Procedures

Previous work (Veregin *et al.*, 1995) indicates that traditional classification methods do not yield high accuracy levels for this dataset. We attribute this to the difficulty of discriminating among classes in feature space due to high within-class variation. Additional work (Sincak *et al.*, 1998) indicates that while non-traditional classifiers can yield enhancements in classification accuracy, the level of enhancement may be small in some cases. The goal of the present study is to enhance the accuracy of these non-traditional classifiers through the application of conflation procedures. The classifiers examined are classification based on fuzzy sets, fuzzy ARTMAP classification and modular neural network classification. Classification based on fuzzy sets — which is distinct from the more common "fuzzy classification" — is adapted from speech recognition applications (Pao, 1989). To our knowledge this technique has not previously been used for image classification purposes. The fuzzy ARTMAP classifier is a supervised classification technique based on Adaptive Resonance Theory and fuzzy sets. It is a model-free approach that generally yields good results regardless of the statistical characteristics of the input data (Carpenter *et al.*, 1992). The modular neural network method has been shown to be capable of approximating complex discriminant functions separating classes in feature space (Haykin, 1994). The theoretical background for these classifiers and our adaptations of them for remote sensing data are described in Sincak *et al.* (1998).

These classifiers were applied to the Mud Run video data using a training set of 4880 pixels for the eight classes. Assessment of classification accuracy was performed using test sites randomly selected from each class. The selection was done independently of training site selection. The test sites were selected such that an equal number of observations was obtained for each class. This stratified-random approach ensures that the sample size for each class is large enough to permit per-class accuracy assessment. All accuracy statistics reported here are based on the classification error matrix. Equations for overall accuracy (percent correctly classified or PCC, as well as the kappa statistic) are presented elsewhere in the literature. (For reviews see Veregin, 1989, and Congalton, 1991.) For computations on test data, equations for stratified-random sampling are used (Fitzpatrick-Lins, 1981; Stehman, 1996).

User's and producer's accuracies (UA and PA, respectively) are also computed. These are per-class accuracy statistics since they refer to only one class. UA is defined as the number of correctly classified pixels in a class divided by the total number of pixels assigned to that class. This gives the probability that a pixel randomly selected from the class on the image is in fact correctly classified. PA is defined as the number of correctly classified pixels in a class divided by the total number of pixels that are actually in that class. This gives the probability that a pixel randomly selected from the class on the ground is in fact correctly classified on the image (Story and Congalton, 1986).

Classification Results

Classification Based on Fuzzy Sets

Figure 2 shows the classified image for subcatchment 24 and Table 1 show the classification error matrix for the test sites. The weighted PCC is 71.3 percent and the weighted kappa statistic is 0.625. UA ranges from a low of 54 percent (shadow) to a high of 96 percent (water). Analysis of the classification error matrix reveals frequent confusion between the concrete, asphalt and shingle roof classes. This is perhaps not surprising, as shingles often have an asphalt base and since concrete and asphalt have a similar appearance, especially after extensive road wear has taken place. There is also evidence of confusion between water, deciduous trees and shadow. Again, this result is not surprising as water and shadow both have low reflectance values, and as areas of deciduous tree cover contain a mixture of tree crowns interspersed with shadows. Compared to traditional classifiers, the fuzzy classifier produces superior results for several classes, especially shingle roofs and grass.

Classification Based on Fuzzy ARTMAP Neural Networks

Figure 3 shows the classified image for subcatchment 24 and Table 2 gives the classification error matrix for the test sites. The weighted PCC is 74.1 percent and the weighted kappa statistic is 0.645. UA ranges from a low of 56 percent (grass) to a high of 93 percent (grass-stubble). PA ranges from a low of 52 percent (grass-stubble) to a high of 96 percent (water). Analysis of the classification error matrix shows confusion between the concrete, asphalt and shingle roof classes, between the water, deciduous tree and shadow

classes, and between the grass and grass-stubble classes. Per-class accuracy statistics are generally higher for the fuzzy ARTMAP approach than for the supervised fuzzy approach.

Classification Based on Modular Neural Network

Results for the modular neural network classifier are quite poor. The classification error matrix (Table 3) shows confusion between almost every class, and the classified image (Figure 4) exhibits high-frequency variation not present in the other classified images or on the ground. Overall accuracy is low (weighted PCC of 42.8 percent and weighted kappa of 0.299). PA ranges from 4 percent (concrete) to 88 percent (deciduous trees), while UA ranges from 7 percent (concrete) to 86 percent (water). Despite the poor performance of this classifier we note that it yields a higher UA for water (86 percent) than either of the other two classifiers. Thus a pixel selected at random from the water class on the modular neural network image has a higher probability of actually being water than a pixel selected from the water class on any other image.

Conflation Procedures

The three classified images presented above are different representations of the same true spatial distribution of land cover classes in the study area. The three images have similar gross patterns of land cover, but crosstabulation of the images indicates that pixel-by pixel agreement is actually quite low. The lowest agreement (between supervised fuzzy and modular neural network approaches) is only 45 percent, and even for those images that are most similar (i.e., supervised fuzzy and fuzzy ARTMAP approaches) agreement is only 74 percent.

To complicate matters, not all classes are portrayed most accurately on the same image. Even when overall accuracy is low, certain classes may still be quite accurate. This effect is shown most conclusively by the fact that the image with the lowest overall accuracy (modular neural network) has the highest UA statistic for the water class. Different classifiers produce different accuracy levels for different classes. Use of overall accuracy statistics (such as PCC and Kappa) can mask significant variations in per-class accuracy values and classifier performance. This suggests that rather than searching for a single optimal classifier that performs well for all classes, it might be more fruitful to fuse those portions of each image that exhibit the highest accuracy to yield a hybrid image that is more accurate than

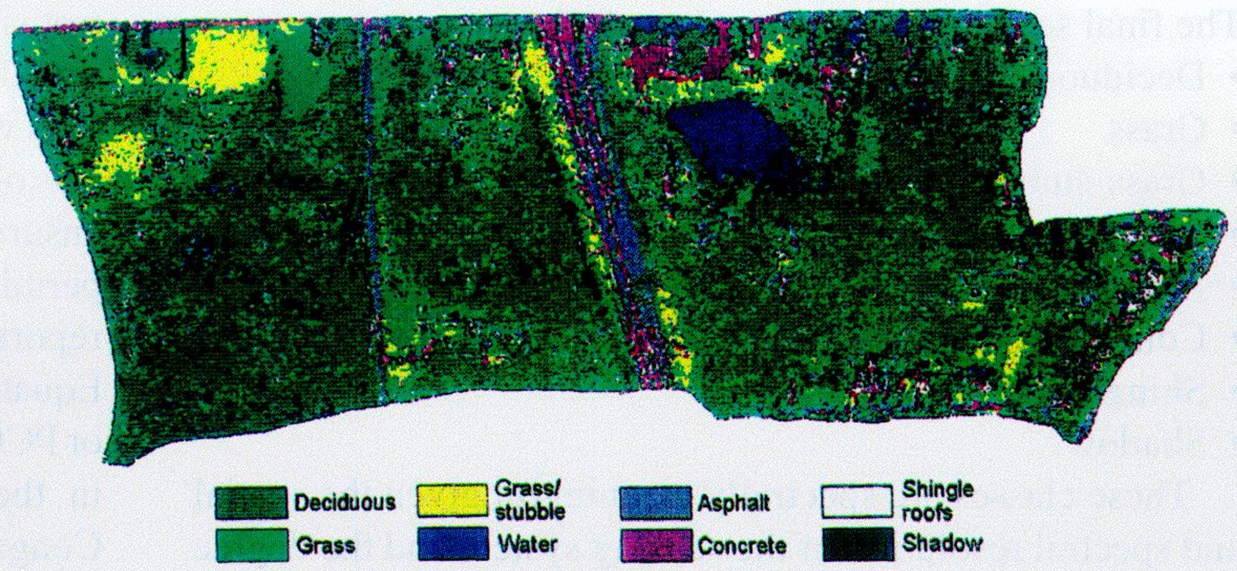

Figure 2 Classified image for classification using fuzzy sets (image 1).

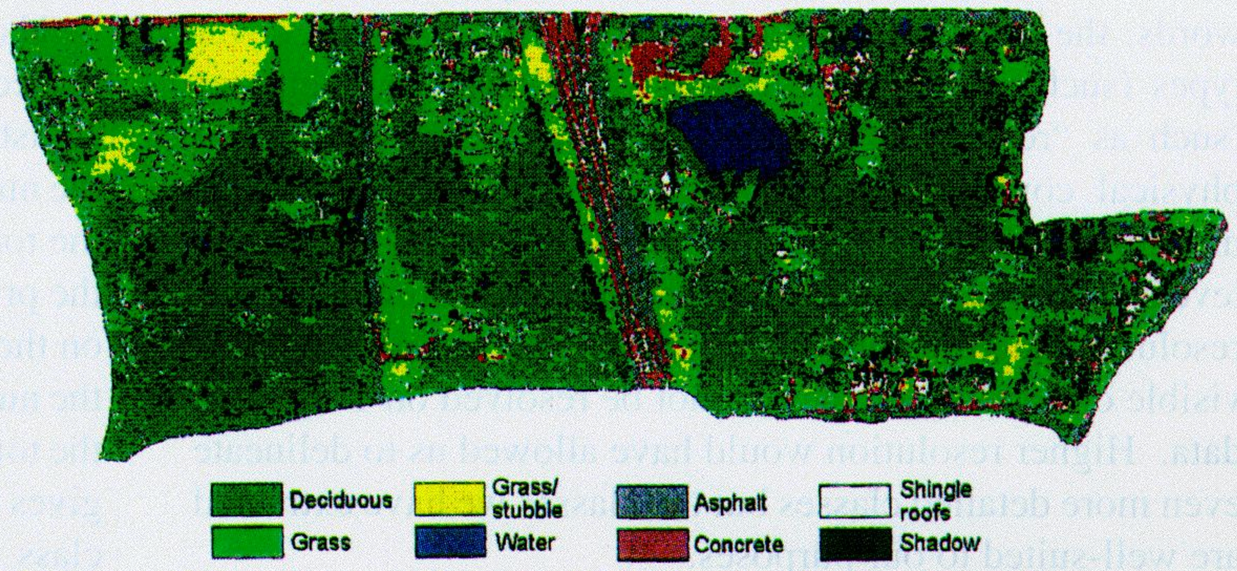

Figure 3 Classified image for fuzzy ARTMAP classification (image 2).

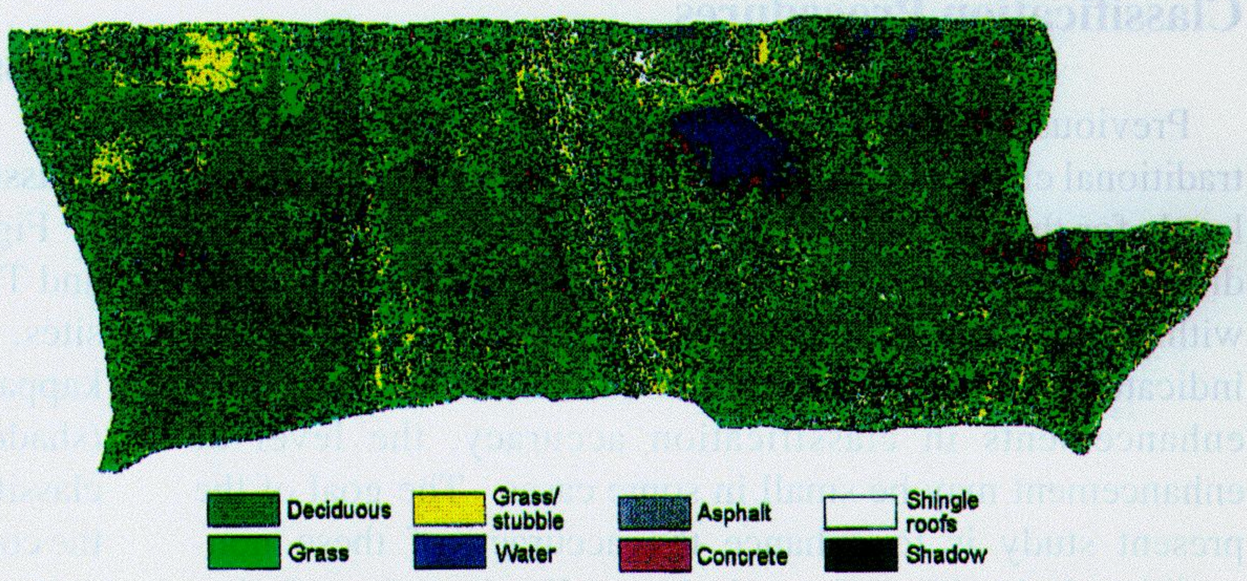

Figure 4 Classified image for modular neural network classification (image 3).

Table 1 Classification error matrix for classification using fuzzy sets (image 1).

Classified image: Rows / Test sites: Columns	Decid. trees	Grass	Grass-stubble	Water	Asphalt	Concrete	Shingle roofs	Shadow	Sum	UA
Deciduous trees	19	1	0	1	1	0	2	4	28	0.68
Grass	1	21	3	0	0	0	0	0	25	0.84
Grass-stubble	0	1	17	0	0	0	0	0	18	0.94
Water	1	0	0	24	0	0	0	7	32	0.75
Asphalt	0	0	2	0	17	3	3	0	25	0.68
Concrete	0	0	1	0	4	18	6	0	29	0.62
Shingle roofs	0	2	2	0	3	4	14	1	26	0.54
Shadow	4	0	0	0	0	0	0	13	17	0.76
Sum	25	25	25	25	25	25	25	25	200	
PA	0.76	0.84	0.68	0.96	0.68	0.72	0.56	0.52		
PCC=0.713 Kappa=0.625										

Table 2 Classification error matrix for fuzzy ARTMAP classification (image 2).

Classified image: Rows Test sites: Columns										
	Decid. trees	Grass	Grass-stubble	Water	Asphalt	Concrete	Shingle roofs	Shadow	Sum	UA
Deciduous trees	21	1	0	1	1	0	1	2	27	0.78
Grass	1	20	11	0	1	0	1	2	36	0.56
Grass-stubble	0	1	13	0	0	0	0	0	14	0.93
Water	0	0	0	24	0	0	0	6	30	0.80
Asphalt	0	1	1	0	18	3	2	0	25	0.72
Concrete	0	0	0	0	5	21	5	0	31	0.68
Shingle roofs	0	2	0	0	0	1	16	1	20	0.80
Shadow	3	0	0	0	0	0	0	14	17	0.82
Sum	25	25	25	25	25	25	25	25	200	
PA	0.84	0.80	0.52	0.96	0.72	0.84	0.64	0.56		
PCC=0.741 Kappa=0.645										

Table 3 Classification error matrix for modular neural network classification (image 3).

Classified image: Rows Test sites: Columns										
	Decid. trees	Grass	Grass-stubble	Water	Asphalt	Concrete	Shingle roofs	Shadow	Sum	UA
Deciduous trees	22	1	0	3	1	1	0	5	33	0.67
Grass	2	10	12	0	3	2	3	2	34	0.29
Grass-stubble	0	2	6	0	9	5	4	0	26	0.23
Water	0	0	0	18	0	0	0	3	21	0.86
Asphalt	0	3	3	0	2	0	1	0	9	0.22
Concrete	0	4	1	1	0	1	4	3	14	0.07
Shingle roofs	0	2	2	0	1	10	5	3	23	0.22
Shadow	1	3	1	3	9	6	8	9	40	0.23
Sum	25	25	25	25	25	25	25	25	200	
PA	0.88	0.40	0.24	0.72	0.08	0.04	0.20	0.36		
PCC=0.428 Kappa=0.299										

any single image. We refer to this process as conflation. The discussion below focuses on two major types of conflation, which we call "heuristic" and "probabilistic."

Heuristic Conflation

The simplest conflation procedures involve simple if-then rules extracted from patterns of misclassification for a set of classified images. The general procedure is as follows.

- First, a frequency distribution of misclassification patterns is generated. A misclassification pattern is of the form $[c_1, c_2, ..., c_n, c']$ where c_i is the class assigned on image i, n is the number of images, and c' is the true class. This information can be extracted from the training set, the test set, or any sample of pixels. The frequency distribution gives the number of occurrences of each misclassification pattern.
- The frequency distribution is converted into a set of if-then rules. Each rule specifies the true class that should be assigned to a pixel when the given misclassification pattern is observed. Note that there may be conflicts that need to be resolved through the use of simple rules. However, our experience shows that there are relatively few of these, largely because misclassification tends to follow systematic patterns.
- The if-then rules are applied to reclassify pixels, creating the conflated image.

Consider an example in which the combination "shadow-shadow-water" (i.e., shadow on image 1, shadow on image 2, and water on image 3) is observed to be consistently associated with a true class of "deciduous trees". In this case an if-then rule is generated that assigns "deciduous trees" to any pixel with the combination "shadow-shadow-water". Note that we are not making this reassignment based on spatial association (i.e., trees cast shadows) but rather on a specific pattern of misclassification across images showing that the combination "shadow-shadow-water" is consistently found to be associated with a true class of "deciduous trees".

Probabilistic Conflation

Probabilistic conflation procedures are based on manipulation of the classification error matrices for each classified image. Several different decision rules can be derived. In each case the derived rules are used to perform reassignment on a pixel-by-pixel basis.

The text below gives a description of each rule and shows a simple example based on the classification error matrices shown in Tables 1 through 3. In this example, assume that a decision is to be made about the class for a pixel that has been classified as "shadow" on image 1, "shadow" on image 2 and "water" on image 3.

Decision Rule 1

This is the simplest of the four rules discussed here. It is based on the selection of the class with the highest UA, as UA measures the accuracy of a class as depicted on the image. For a given pixel, UA is determined for the class that is observed at that pixel location on each of the images. The class corresponding to the highest UA is selected as the conflated result.

Example

UA, shadow, image 1: 13/17 = 0.765
UA, shadow, image 2: 14/17 = 0.824
UA, water, image 3: 18/21 = 0.857
According to rule 1, "water" would be selected.

Decision Rule 2

This rule is based on accumulation of confirmatory evidence (Tikunov, 1986). Confirmation occurs when the same class occurs for a given pixel on more than one image. Accumulation of evidence is performed in the following manner. First, for each image on which the class is observed at the pixel location, we compute the probability of misclassification for the class. This is computed simply as one minus UA. The product of these probabilities (accumulated misclassification) is then computed. The same procedure is applied for the classes observed at the pixel location on the other images, and the accumulated misclassifications are then converted into accumulated UAs by computing one minus the accumulated misclassifications. The conflated result is then the class for which the value of accumulated UA is the highest.

Example

Accumulated UA for water: $1-(1-18/21)=0.857$
Accumulated UA for shadow: $1-(1-13/17)(1-14/17)=0.959$
According to rule 2, "shadow" would be selected.

Decision Rule 3

The third rule involves first converting all elements in each classification error matrix into probabilities by dividing them by their corresponding row totals. Given a pixel assigned to class i by a classification procedure, we use the probabilities in row i of the classification error matrix to determine the probability of observing each class based on the fact that class i was observed on the image. The probabilities for each class are accumulated (see Rule 2) and the class with the highest probability is then selected as the conflated result.

Example

For image 1, given a pixel classified as shadow:
Probability of deciduous trees: 4/17 = 0.235
Probability of shadow: 13/17 = 0.765
Probability of all other classes: 0.0

For image 2, given a pixel classified as shadow:
Probability of deciduous trees: 3/17 = 0.176
Probability of shadow: 14/17 = 0.824
Probability of all other classes: 0.0

For image 3, given a pixel classified as water:
Probability of water: 18/21 = 0.857
Probability of shadow: 3/21 = 0.143
Probability of all other classes: 0.0

Accumulated probability for shadow:
$1-(1-13/17)(1-14/17)(1-3/21)=0.964$

Accumulated probability for water:
$1-(1-0)(1-0)(1-18/21)=0.857$

Accumulated probability for deciduous trees:
$1-(1-4/17)(1-3/17)(1-0)=0.370$

Accumulated probability of all other classes is 0.0

According to rule 3, "shadow" would be selected.

Decision Rule 4

The first three rules account only for errors of commission, since errors of omission do not affect UA. Thus these methods favor classes that are conservatively assigned. Decision rule 4 accounts for both errors of omission and commission. This decision rule is based on the creation of a collapsed classification error matrix. For class i on a given classified image, the collapsed table is a two-by-two table showing pixels as belonging to class i or not class i. The PCCs from the collapsed tables can then be compared for all classes observed at a given pixel location, and the class with the highest PCC is selected as the conflated result. Note that this approach assumes that each class is approximately equally represented in the classification error matrix; if this is not the case then classes with small numbers of pixels will appear to be more accurately classified when the tables are collapsed.

Example

Tables 4a-c show the collapsed classification error matrices for shadow on image 1, shadow on image 2 and water on image 3.

According to rule 4, "water" would be selected.

Conflation Results

For the images examined in this study, heuristic conflation is superior to probabilistic conflation. All conflation techniques yield improvements in accuracy, but the heuristic method produces an increase of 15 percent in overall accuracy relative to the best of the original classified images. The conflated image for the heuristic approach is shown in Figure 5 and the classification error matrix is shown in Table 5.

Table 4a Collapsed classification error matrix, shadow, image 1.

Classified image: Rows	**Test sites: Columns**	
	Shadow	Not Shadow
Shadow	13	4
Not Shadow	12	171
PCC=0.92		

Table 4b Collapsed classification error matrix, shadow, image 2.

Classified image: Rows	**Test sites: Columns**	
	Shadow	Not Shadow
Shadow	14	3
Not Shadow	11	172
PCC=0.93		

Table 4c Collapsed classification error matrix, water, image 3.

Classified image: Rows	**Test sites: Columns**	
	Shadow	Not Shadow
Shadow	18	3
Not Shadow	7	172
PCC=0.95		

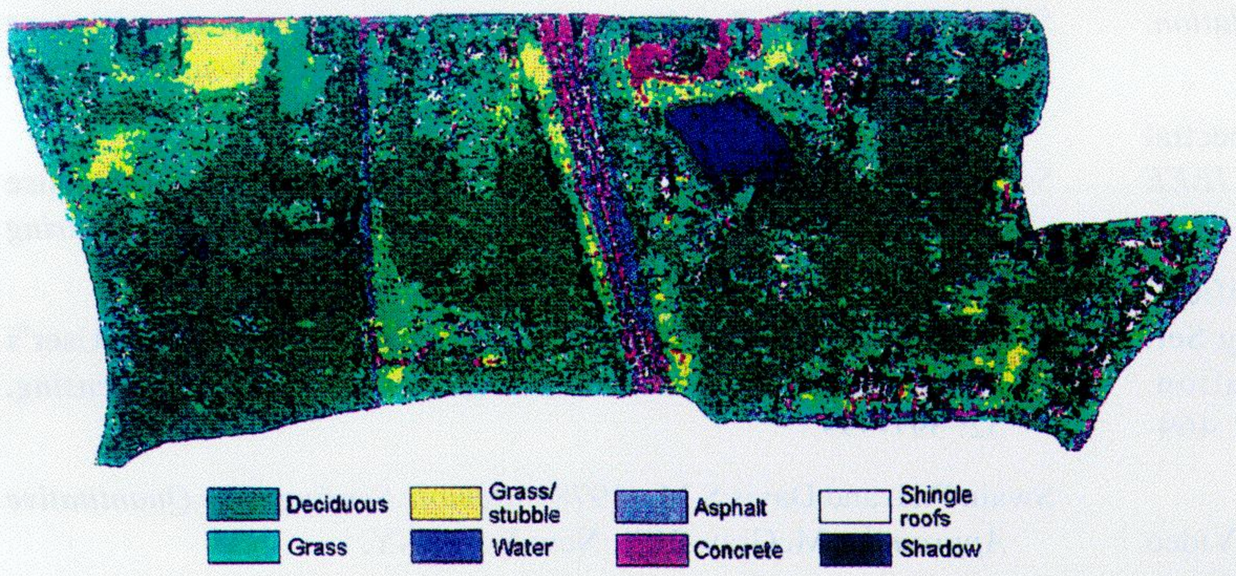

Figure 5 Classified image for heuristic conflation

Table 5 Classification error matrix for heuristic conflation.

Classified image: Rows Test sites: Columns										
	Decid. trees	Grass	Grass-stubble	Water	Asphalt	Concrete	Shingle roofs	Shadow	Sum	UA
Deciduous trees	22	0	0	1	0	0	1	0	24	0.92
Grass	1	23	1	0	0	0	0	0	25	0.92
Grass-stubble	0	1	23	0	0	0	0	0	24	0.96
Water	0	0	0	24	0	0	0	3	27	0.89
Asphalt	0	0	1	0	23	1	2	0	27	0.85
Concrete	0	0	0	0	2	23	3	0	28	0.82
Shingle roofs	0	1	0	0	0	1	19	0	21	0.90
Shadow	2	0	0	0	0	0	0	22	24	0.92
Sum	25	25	25	25	25	25	25	25	200	
PA	0.88	0.92	0.92	0.96	0.92	0.92	0.76	0.88		
PCC=0.908 Kappa=0.871										

Note the high overall accuracy levels and the high per-class accuracy statistics for all classes.

Cross-tabulation of the various conflated results with the three original classified images shows that conflation has a significant impact on classification results. Agreement ranges from a high of 88 percent (fuzzy ARTMAP vs. probabilistic conflation rule 3) to a low of 46 percent (modular neural network approach vs. probabilistic conflation rule 3). Agreement between the probabilistic (rule 3) and heuristic conflation results is 81 percent, which indicates that the two conflation methods also produce somewhat different results.

Conclusion

This study demonstrates that conflation procedures offer the possibility of significant enhancements in classification accuracy when multiple land cover classifications have been produced for the same area. Conflation procedures can be developed easily using information available from the classification error matrix and implemented as a post-processing step. The rationale for conflation is that no single image necessarily classifies all classes with equal accuracy. Conflation allows the user to select those parts of each image that are most accurately classified and merge these together to create a hybrid image. (Conflation is of course unnecessary if one classification result has the highest per-class accuracy statistics for all classes.) It is likely that more elaborate conflation procedures can be developed and we urge other researchers to examine this issue in more detail. Our own research in this area is currently focusing on the development of methods to identify the most appropriate conflation methods to use in different contexts, as different methods can yield different results.

Acknowledgments

This paper is based on work sponsored by the U.S.-Slovak Science and Technology Joint Fund in Cooperation with the Ministry of Ecology of the Slovak Republic and the US Environmental Protection Agency under Project Number 94077.

References

Baldwin, J.F., Martin, T.P. and Pilsworth, B.W. 91995). *Fril—Fuzzy and Evidential Reasoning in Artificial Intelligence*. John Wiley and Sons, New York NY.

Benediktsson, J., Swain, P. and Ersoy, O. (1990). Neural Network Approaches Versus Statistical Methods in Classification of Multisource Remote Sensing Data. *IEEE Transactions on Geoscience and Remote Sensing*, 28(4): 540-552.

Carpenter, G.A., Gjaja, M., Gopal, S. and Woodcock, C. (1997). ART Neural Networks for Remote Sensing: Vegetation Classification from Landsat TM and Terrain Data. *IEEE Transactions on Geoscience and Remote Sensing*, 35(2): 308-325.

Civco D.L. and Wang Y. (1994). Classification of Multispectral, Multitemporal, Multisource Spatial Data Using Artificial Neural Networks: *ACSM/ASPRS Annual Convention and Exposition*, Baltimore, 1: 123-133

Congalton, R.G. (1991). A Review of Assessing the Accuracy of Classifications of Remotely Sensed Data. *Remote Sensing of Environment*, 37: 35-46.

Cushnie, J.L. (1987). The Interactive Effect of Spatial Resolution and Degree of Internal Variability Within Land Cover Types on Classification Accuracies. *International Journal of Remote Sensing* 8: 15-29.

Fitzpatrick-Lins, K. (1981). Comparison of Sampling Procedures and Data Analysis for a Land-use and Land-cover Map. *Photogrammetric Engineering and Remote Sensing*, 47: 343-351.

Foody, G.M., McCulloch, M.B. and Yates, W.B. (1995). Classification of Remotely Sensed Data by an Artificial Neural Network: Issues Related to Training Data Characteristics. *Photogrammetric Engineering and Remote Sensing*, 61: 391-401.

Goodchild, M.F. (1996). Conflation: Combining GIS Sources, Internet URL:\\http://www.ncgia.ucsb.edu/research/ucgis/proposals/conflation.html

Haykin, S. (1994). *Neural Networks: A Comprehensive Foundation.* Macmillan, New York N Y.

Heerman P.D. and Khazenie N. (1992). Classification of Multispectral Remote Sensing Data Using a BP Neural Network. *IEEE Transactions on Geoscience and Remote Sensing*, 30(1): 81-88.

Hepner, G., Logan, T., Rittne, N. and Bryant, N. (1990). Artificial Neural Network Classification Using a Minimum Training Set: Comparison to Conventional Supervised Classification. *Photogrammetric Engineering and Remote Sensing*, 56: 469-473.

King, D.J. (1995). Airborne Multispectral Digital Camera and Video Sensors: A Critical Review of System Designs and Applications. *Canadian Journal of Remote Sensing*, 21(3): 245-273.

Kulkarni A. (1994). *Artificial Neural Networks for Image Understanding.* Van Nostrand Reinhold, New York NY.

Lee, T., Richards, J.A. and Swain, P.H. (1987). Probabilistic and Evidential Approaches for Multisource Data Analysis. *IEEE Transactions on Geoscience and Remote Sensing* 25(3): 283-293.

Lin, C. and Lee, C. (1996). *Neural Fuzzy Systems.* Prentice Hall, Englewood Cliffs NJ.

Markham, B.L. & Townshend, J.R.G. (1981). Land Cover Classification Accuracy as a Function of Sensor Spatial Resolution. *Fifteenth International Symposium on Remote Sensing of Environment*: 1075-1090.

Ocelikova, E. (1993). Clustering Analysis as a Classification Tool. *International Scientific Conference on Micro-Cad Systems 93*, Kosice, Slovak Republic.

Ocelikova, E. (1994). Significance of Cluster Analysis. *Proceedings of 1st IFAC Workshop on New Trends in Design of Control Systems*, 420-423.

Pao, T. (1989). *Adaptive Pattern Recognition and Neural Networks*: Addison-Wesley, Reading MA.

Sincak, P., Veregin, H. & Kopco, N. (1998). Computational intelligence for classification of remotely sensed images. *Neural Network World*, 8(5), 577-594.

Stehman, S. (1996). Estimating the Kappa Coefficient and its Variance under Stratified Random Sampling. *Photogrammetric Engineering and Remote Sensing*, 62: 401-408.

Story, M. and Congalton, R. (1986). Accuracy Assessment: A User's Perspective. *Photogrammetric Engineering and Remote Sensing*, 52: 397-399.

Swain P.H. and Davis S.M. (1978). *Remote Sensing: The Quantitative Approach.* McGraw-Hill, New York, NY.

Tikunov, V.S. (1986). *Some Issues in the Modeling Approach to Cartography.* Unpublished manuscript, Department of Geography, University of California, Santa Barbara.

Toll, D.L. (1985). Effect of Landsat Thematic Mapper Sensor Parameters on Land Cover Classification. *Remote Sensing of Environment* 17: 129-140.

Tou J. and Gonzales, R. (1974). *Pattern Recognition Principles.* Addison-Wesley, Reading MA.

Veregin, H. (1989). *A Taxonomy of Error on Spatial Databases.* Technical paper 89-12, National Center for Geographic Information and Analysis, University of California, Santa Barbara.

Veregin, H., Sincak, P., Gregory, K. and Davis, L. (1995). Integration of High Resolution Video Imagery and Urban Stormwater Runoff Modeling. *15th Biennial Workshop on Videography and Color Photography in Resource Assessment*, 182-191.

Wang F. (1990). Fuzzy Supervised Classification of Remote Sensing Images, *IEEE Transactions on Geoscience and Remote Sensing*, 28: 194-201.

Wilkinson G.G. (1995). Classification Algorithm - Where Next? *Proceedings of the International Workshop on SoftComputing in Remote Sensing Data Analysis*, Milan, Italy, 93-99.